Origin of high open-circuit voltage in a planar heterojunction solar cell containing a non-fullerene acceptor

Nongyi Cheng,[1] Yuelin Peng,[2] and Trisha L. Andrew[3,a)]
[1]*Department of Chemistry, University of Wisconsin-Madison, Madison, Wisconsin 53706, USA*
[2]*Department of Electrical and Computer Engineering, University of Wisconsin-Madison, Madison, Wisconsin 53706, USA*
[3]*Department of Chemistry and Chemical Engineering, University of Massachusetts Amherst, Amherst, Massachusetts 01003, USA*

(Received 25 July 2017; accepted 13 September 2017; published online 25 September 2017)

Vapor-deposited, planar heterojunction organic solar cells containing a periflanthene donor and either a fullerene or non-fullerene acceptor are investigated. A high V_{OC} of 1.16 V is observed in devices containing the non-fullerene, pyrrolo[3,4-c]pyrrole-1,4-dione, 3,6-bis(4-chlorophenyl)-2,5-dihydro acceptor, whereas analogous devices containing C_{60} only result in a V_{OC} of 0.8 V. The measured band energy levels of the two different acceptors do not readily explain the observed difference. Small-perturbation transient photovoltage and transient photocurrent measurements reveal that interfacial charge recombination is comparatively slower for the non-fullerene acceptor, resulting in relatively higher V_{oc} values. *Published by AIP Publishing.*
[http://dx.doi.org/10.1063/1.4997502]

Developing fullerene alternatives for use in organic solar cells (OSCs) is attracting contemporary research interest. Although fullerenes are pervasive electron-accepting components in many heterojunction solar cells, longstanding disadvantages, such as weak visible/near-infrared light absorption, oxygen sensitivity, and a small range of available energy levels, have become increasingly limiting factors for efficiency optimization and large-scale OSC production.[1]

Selected compounds have recently been reported as competitive alternatives to fullerene acceptors in OSCs.[2–6] We also reported a vapor-deposited solar cell containing tetraphenyldibenzoperiflanthene (DBP) as a donor and pyrrolo[3,4-c]pyrrole-1,4-dione, 3,6-bis(4-chlorophenyl)–2,5-dihydro (DPP) as a non-fullerene acceptor (Fig. 1).[7] This solar cell had a notably high open circuit voltage (V_{oc}) of 1.16 V, compared to a V_{oc} of 0.89 V for an analogous device containing C_{60}. Reports of single-junction solar cells with open circuit voltages higher than 1 V are limited.[5] Therefore, we sought to elucidate the physical origin of the unusually high open circuit voltage observed for our DBP/DPP solar cell and explain why differences in V_{OC} are observed between C_{60} and DPP acceptors.

The maximum achievable open circuit for a particular donor-acceptor heterojunction can be predicted using the formula: $V_{oc} = \Delta E_{DA} - 0.3$ V, where ΔE_{DA} is the energy difference between the LUMO (or conduction band) of the acceptor and the HOMO (or valence band) of the donor.[8] In practice, additional factors other than ΔE_{DA} can further attenuate V_{oc}, including reverse saturation currents,[9] electrode/active layer interfaces,[10,11] energetic disorder in active layers,[12] charge transfer states,[13] and organic heterointerface morphology.[14] The energy levels of all the layers in both DBP/DPP and DBP/C_{60} devices are previously reported[7] and shown in Fig. 1. The DBP/DPP interface has a ΔE_{DA} of 1.3 eV, and DBP/C_{60} has a comparable ΔE_{DA} of 1.5 eV. Therefore, band energy offsets alone cannot satisfactorily explain the origin of high open circuit voltage in DBP/DPP solar cells.

Recombination is the main conduit for energy loss in OSCs, and the role of charge recombination in limiting V_{oc} has been widely studied.[15–18] Hypothesizing that charge recombination, or lack thereof, during device operation was the origin of the high V_{OC} observed for DPP-based solar cells, we used small-perturbation transient photovoltage (TPV) and transient photocurrent (TPC) measurements to study charge recombination dynamics in DBP/DPP and DBP/C_{60} devices.[19] TPV was performed to measure the lifetimes of the transient charge carrier induced by pulsed light at different background light intensities. TPC was performed to measure the transient charge

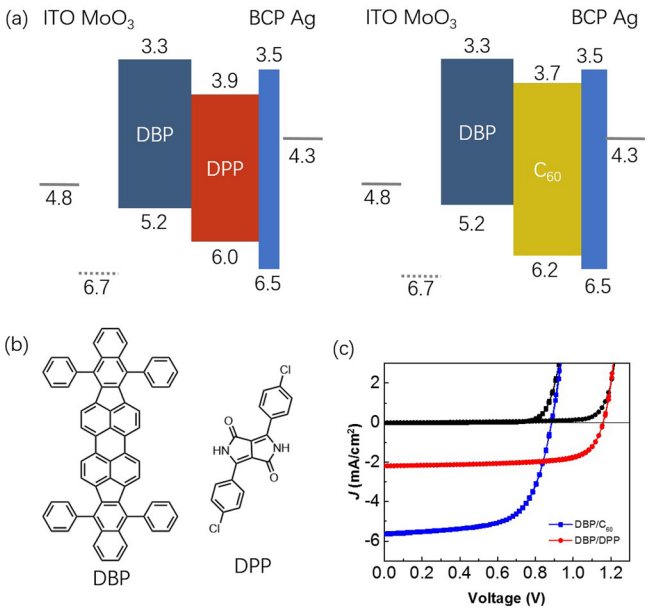

FIG. 1. (a) Energy levels of each layer in DBP/DPP and DBP/C_{60} solar cells. (b) Chemical structures of DBP and DPP. (c) Current density-voltage curves of DBP/DPP and DBP/C_{60} solar cells.

a)tandrew@umass.edu

carrier densities. By combining the two measurements, the recombination rate of the charge carriers at the donor/acceptor interface can be calculated.

J-V curves for DBP/DPP and DBP/C_{60} solar cells under AM1.5 simulated sunlight (100 mW/cm^2) are shown in Fig. 1(c). The DBP/DPP device exhibited a V_{oc} of 1.16 V, a short circuit current density (J_{sc}) of 2.19 mA/cm^2, and a fill factor of 0.70. The DBP/C_{60} device exhibited a V_{oc} of 0.89 V, a J_{sc} of 5.64 mA/cm^2, and a fill factor of 0.65. Both the V_{oc} and the fill factor of the DBP/DPP device were higher than those of the DBP/C_{60} device. The comparatively small J_{sc} of the DBP/DPP device can be attributed to weak, wavelength-restricted (400–600 nm) light absorption in DPP.[7]

TPV measurements were first performed to probe free charge carrier lifetimes (τ_n) at different open circuit voltages. The device was held at an open circuit under a continuous background white light. Different V_{oc} values were obtained by adjusting the strength of the white light. Once the device reached the steady state, it had a fixed charge density, n, and a steady V_{oc}. A pulsed LED light was then applied to the device to induce a small, transient increase in charge carrier density (Δn) and, therefore, a transient photovoltage (ΔV). The transient voltage thus created decayed back to the original open circuit voltage value at the end of each light pulse. The intensity of pulsed light was regulated to keep ΔV smaller than 20 mV, thus ensuring that Δn was a small perturbation compared to n. Under this condition, ΔV is proportional to Δn and the charge carrier decay follows a pseudo first-order rate:

$$\Delta V = \Delta V_0 e^{-t/\tau_{\Delta n}}, \tag{1}$$

$$\Delta n = \Delta n_0 e^{-t/\tau_{\Delta n}}, \tag{2}$$

where t is the time, ΔV_0 and Δn_0 are the transient photovoltage and the change in charge carrier density at $t = 0$, respectively, and $\tau_{\Delta n}$ is the lifetime of the transient.

Transient photovoltage decays of DBP/C_{60} and DBP/DPP devices at different background light intensities are shown in Fig. 2. The charge carrier lifetimes in both devices decreased as background white light intensity increased. This behavior means that charge carrier decay dynamics exhibit a charge density dependence with an order higher than one. It can also be seen from the graph that the charge carrier lifetime in the DBP/DPP device was one order of magnitude higher than that in the DBP/C_{60} device.

Charge carrier densities (n) in the devices at an open circuit can be determined using the TPV results and TPC measurements. To perform TPC measurements, the device was illuminated with the same background white light and the same pulsed green light as in the TPV measurement to keep n and Δn consistent between the two measurements. The device was held at a short circuit, and the current flowing through the device was measured using a current-voltage convertor and an oscilloscope. Assuming that all photogenerated charges were collected at the short circuit and that charge generation was independent of the electric field, the amount of transient photogenerated charges (Δq) can be obtained by integrating the photocurrent transient over time. To determine the steady-state carrier density (n) at the open circuit, the concept of differential capacitance was invoked:

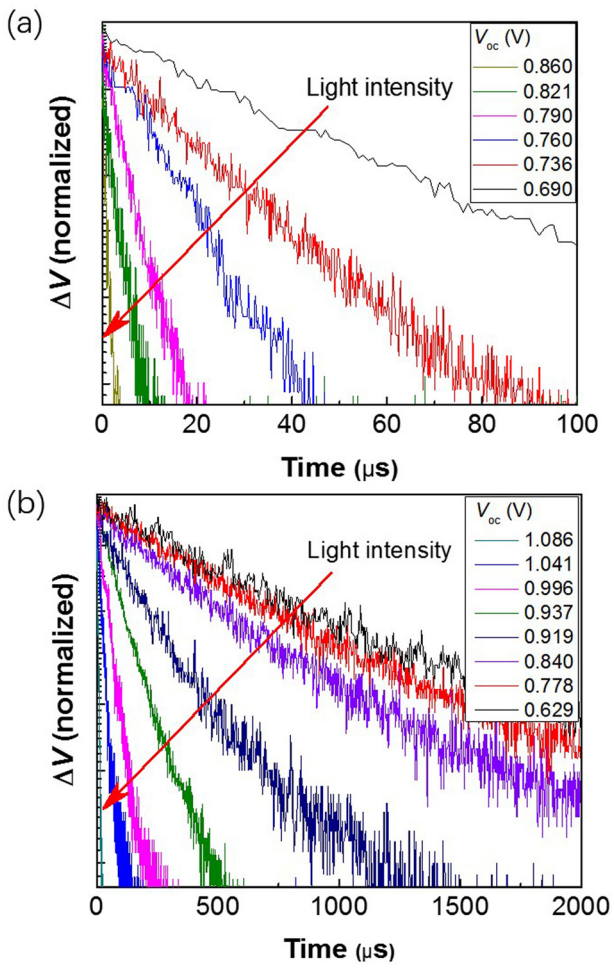

FIG. 2. Transient photovoltage decays of (a) DBP/C_{60} and (b) DBP/DPP devices at different background white light intensities.

$$dC\,(V_{oc}) = \Delta q/\Delta V(V_{oc}), \tag{3}$$

where $dC(V_{oc})$ and $\Delta V(V_{oc})$ are the differential capacitance and transient photovoltage at a certain V_{oc}. In Eq. (3), Δq and $\Delta V(V_{oc})$ were obtained from TPC and TPV measurements, respectively. The total amount of charge in the device at a particular V_{oc} can be calculated by integrating dC over V_{oc} [Figs. 3(a) and 3(c)]:

$$q(V_{oc}) = \int_0^{V_{oc}} dC(V_{oc})dV_{oc}, \tag{4}$$

$$n = q/eA, \tag{5}$$

where q is the total amount of charge in the device at open circuit voltage V_{oc}, e is the elementary charge, and A is the total device area.

To establish the rate law for charge carrier recombination, the transient charge carrier lifetime ($\tau_{\Delta n}$) is plotted against n [Figs. 3(b) and 3(d)]. The recombination follows a pseudo first order rate law

$$dn/dt = -k_n n = -n/\tau_n, \tag{6}$$

where

$$k_n = 1/\tau_n = kn^{\lambda}, \tag{7}$$

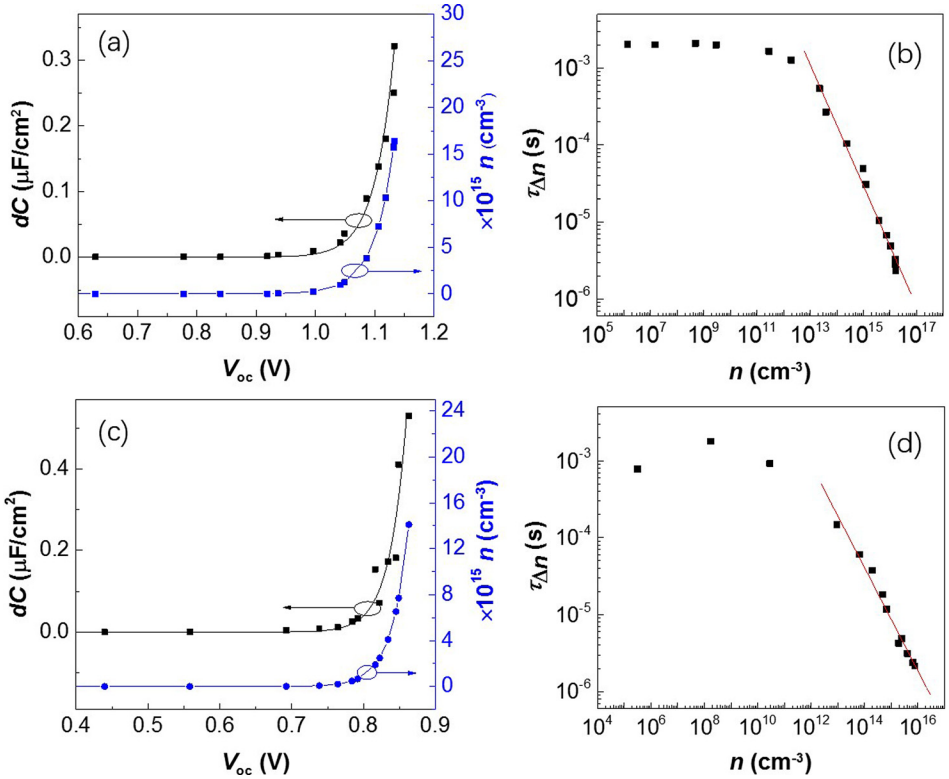

FIG. 3. Plots of differential capacitance and charge carrier densities as a function of V_{oc} in (a) DBP/DPP and (c) DBP/C_{60} devices. Transient photogenerated charge carrier lifetime ($\tau_{\Delta n}$) as a function of charge carrier density for (b) DBP/DPP and (d) DBP/C_{60} devices. $\tau_{\Delta n}$ is found to decay exponentially as a function of n at high n values.

where k_n and k are the charge density-dependent and independent rate coefficients, respectively, and τ_n is the charge density-dependent charge carrier lifetime. If the perturbation, Δn, is small compared to n, it can be derived that[14]

$$\tau_{\Delta n} = \frac{1}{1+\lambda}\,\tau_n. \tag{8}$$

By substituting Eq. (7) into Eq. (8), we find that

$$\tau_{\Delta n} = \frac{1}{k(1+\lambda)}\,n^{-\lambda}. \tag{9}$$

From Figs. 3(b) and 3(d), it is evident that $\tau_{\Delta n}$ decreases exponentially with n at high n values in both devices. At low charge carrier densities, $\tau_{\Delta n}$ is constant for both DBP/C_{60} and DBP/DPP devices. We suggest that this is because geminate recombination is dominant in both devices at low charge carrier densities. By fitting the curves at high n values, we obtained λ values of 0.79 for the DBP/DPP device and 0.57 for the DBP/C_{60} device. The recombination rates for DBP/DPP and DBP/C_{60} devices were found to be $k_A n^{1.79}$ and $k_B n^{1.67}$, respectively, where $k_A = 3.1 \times 10^{-8}$ and $k_B = 6.0 \times 10^{-6}$. In both devices, the exponent is close to 2, which means that bimolecular recombination is dominant under the open circuit condition in both devices. However, the DBP/DPP device exhibits a recombination constant k that is two orders of magnitude smaller than the DBP/C_{60} device.

To further prove that the main factor limiting V_{oc} in these devices is charge recombination, we compared the flux of photogenerated charge (J_{gen}) and the calculated charge recombination (J_{rec}) at the open circuit based on the above results. We assumed that, at the short circuit, all photogenerated charges were collected by the electrodes and charge generation was independent of the electric field within the device, i.e., $J_{gen} \approx J_{sc}$. We calculated J_{rec} values at the open circuit using

$$J_{rec} = edkn^{1+\lambda}, \tag{10}$$

where e is the elementary charge, d is the thickness of the active layer, and $kn^{1+\lambda}$ is the rate of recombination; n can be obtained from the data presented in Figs. 3(a) and 3(c). J_{rec} values at V_{oc} were calculated to be 2.10 mA/cm^2 and 5.37 mA/cm^2 for the DBP/DPP and DBP/C_{60} devices, respectively. In both devices, the calculated J_{rec} values at V_{oc} are close to their J_{sc}, that is, $J_{rec} \approx J_{loss}$ at the open circuit. This confirms that the main loss of current at the open circuit is charge recombination.

In conclusion, we used TPV and TPC techniques to study the recombination dynamics in the high open-circuit voltage DBP/DPP solar cell and an analogous DBP/C_{60} solar cell. We found that bimolecular recombination was dominant at high voltages in both devices, but the recombination rate constant for the DBP/DPP device was two orders of magnitude smaller than that for the DBP/C_{60} device. We concluded that the high open-circuit voltage of the DBP/DPP device originated from this decreased recombination rate. Our results suggest that optimizing the performance of solar cells containing non-fullerene acceptors will require increasing the lifetimes of the free charge carriers, in addition to tailoring the energy levels of the active layers.

All chemicals were used without any further purification after purchase. The devices were fabricated with the following structures: MoO_3 (5 nm)/DBP (25 nm)/DPP (15 nm)/BCP (7.5 nm)/Ag (100 nm). Pre-patterned ITO coated glass was cleaned as follows before use: sonicated in detergent solution, rinsed with DI water followed by acetone for 5 min, and dipped into boiling isopropanol for 5 min (2×). MoO_3 (Sigma Aldrich), DBP (Lumtec), DPP (TCI), BCP (Sigma Aldrich),

C_{60} (Sigma Aldrich), and silver (99.99%, Kurt J. Lesker) were deposited through thermal evaporation under vacuum ($<10^{-6}$ Torr). All *J-V* curves were measured in the dark and under 100 mW/cm^2 white illumination (LCS-100, Oriel) using a Keithley 6487.

TPV and TPC techniques have been reported in the previous literature.[19] In the TPV measurement, the device was illuminated with a continuous background white light and held at the open circuit by connecting to the 1 MΩ input of an oscilloscope (Tektronix TDS 3054B). A green LED (525 nm, Everlight) was pulsed by an Agilent 33220A 20 MHz function/arbitrary waveform generator. The voltage transient caused by the pulsed LED was measured using the oscilloscope. In the TPC measurement, the device was illuminated with the same background white light and the same pulsed green light but was held at the short circuit. The short circuit was held by connecting to a current-voltage convertor with a feedback resistor of 100 kΩ. The voltage transient from the current-voltage convertor was measured using a Tektronix oscilloscope and converted into a current transient using Ohm's Law.

This work was funded by the Air Force Office of Scientific Research (Grant number FA9550–14-1–0128).

[1]G. Sauvé and R. Fernando, J. Phys. Chem. Lett. **6**, 3770 (2015).
[2]Z. Mao, W. Senevirathna, J. Y. Liao, J. Gu, S. V. Kesava, C. Guo, E. D. Gomez, and G. Sauvé, Adv. Mater. **26**, 6290 (2014).
[3]H. Bin, Y. Yang, Z.-G. Zhang, L. Ye, M. Ghasemi, S. Chen, Y. Zhang, C. Zhang, C. Sun, L. Xue, C. Yang, H. Ade, and Y. Li, J. Am. Chem. Soc. **139**, 5085 (2017).
[4]S. Li, Z. Zhang, M. Shi, C.-Z. Li, and H. Chen, Phys. Chem. Chem. Phys. **19**, 3440 (2017).
[5]D. Baran, T. Kirchartz, S. Wheeler, S. Dimitrov, M. Abdelsamie, J. Gorman, R. S. Ashraf, S. Holliday, A. Wadsworth, N. Gasparini, P. Kaienburg, H. Yan, A. Amassian, C. J. Brabec, J. R. Durrant, and I. McCulloch, Energy Environ. Sci. **9**, 3783 (2016).
[6]K. Cnops, B. P. Rand, D. Cheyns, B. Vereet, M. A. Empl, and P. Heremans, Nat. Commun. **5**, 3406 (2014).
[7]Y. Peng, L. Zhang, and T. L. Andrew, Appl. Phys. Lett. **105**, 083304 (2014).
[8]M. C. Scharber, D. Mühlbacher, M. Koppe, P. Denk, C. Waldauf, A. J. Heeger, and C. J. Brabec, Adv. Mater. **18**, 789 (2006).
[9]W. J. Potscavage, A. Sharma, and B. Kippelen, Acc. Chem. Res. **42**, 1758 (2009).
[10]A. Tada, Y. Geng, M. Nakamura, Q. Wei, K. Hashimoto, and K. Tajima, Phys. Chem. Chem. Phys. **14**, 3713 (2012).
[11]E. L. Ratcliff, A. Garcia, S. A. Paniagua, S. R. Cowan, A. J. Giordano, D. S. Ginley, S. R. Marder, J. J. Berry, and D. C. Olson, Adv. Energy Mater. **3**, 647 (2013).
[12]G. Garcia-Belmonte and J. Bisquert, Appl. Phys. Lett. **96**, 113301 (2010).
[13]T. M. Burke, S. Sweetnam, K. Vandewal, and M. D. McGehee, Adv. Energy Mater. **5**, 1500123 (2015).
[14]M. D. Perez, C. Borek, S. R. Forrest, and M. E. Thompson, J. Am. Chem. Soc. **131**, 9281 (2009).
[15]C. G. Shuttle, B. O'Regan, A. M. Ballantyne, J. Nelson, D. D. C. Bradley, and J. R. Durrant, Phys. Rev. B **78**, 113201 (2008).
[16]A. Maurano, R. Hamilton, C. G. Shuttle, A. M. Ballantyne, J. Nelson, B. O'Regan, W. Zhang, I. McCulloch, H. Azimi, M. Morana, C. J. Brabec, and J. R. Durrant, Adv. Mater. **22**, 4987 (2010).
[17]D. Credgington, R. Hamilton, P. Atienzar, J. Nelson, and J. R. Durrant, Adv. Funct. Mater. **21**, 2744 (2011).
[18]D. Credgington, Y. Kim, J. Labram, T. D. Anthopoulos, and J. R. Durrant, J. Phys. Chem. Lett. **2**, 2759 (2011).
[19]A. Maurano, C. G. Shuttle, R. Hamilton, A. M. Ballantyne, J. Nelson, W. Zhang, M. Heeney, and J. R. Durrant, J. Phys. Chem. C **115**, 5947 (2011).